Development 127, 3877-3888 (2000)
Printed in Great Britain © The Company of Biologists Limited 2000
DEV0315

Auxin and *ETTIN* in *Arabidopsis* gynoecium morphogenesis

Jennifer L. Nemhauser*, Lewis J. Feldman and Patricia C. Zambryski*

Department of Plant and Microbial Biology, 111 Koshland Hall, University of California, Berkeley, CA 94720-3102, USA
*Authors for correspondence (e-mail: zambrysk@nature.berkeley.edu and jnemhaus@nature.berkeley.edu)

Accepted 3 July; published on WWW 22 August 2000

SUMMARY

The phytohormone auxin has wide-ranging effects on growth and development. Genetic and physiological approaches implicate auxin flux in determination of floral organ number and patterning. This study uses a novel technique of transiently applying a polar auxin transport inhibitor, N-1-naphthylphthalamic acid (NPA), to developing *Arabidopsis* flowers to further characterize the role of auxin in organogenesis. NPA has marked effects on floral organ number as well as on regional specification in wild-type gynoecia, as defined by morphological and histological landmarks for regional boundaries, as well as tissue-specific reporter lines. NPA's effects on gynoecium patterning mimic the phenotype of mutations in *ETTIN*, a member of the auxin response factor family of transcription factors. In addition, application of different concentrations of NPA reveal an increased sensitivity of weak *ettin* alleles to disruptions in polar auxin transport. In contrast, the defects found in *spatula* gynoecia are partially rescued by treatment with NPA. A model is proposed suggesting an apical-basal gradient of auxin during gynoecium development. This model provides a mechanism linking ETTIN's putative transcriptional regulation of auxin-responsive genes to the establishment or elaboration of tissue patterning during gynoecial development.

Key words: *Arabidopsis thaliana*, Gynoecium, Patterning, Polar auxin transport, N-1-naphthylphthalamic acid, NPA, *ETTIN*, *SPATULA*, Flower development

INTRODUCTION

A fundamental question in developmental biology is the origin of complex patterns. Ornate yet eminently reproducible systems mold the form and function of every tissue and organ. One of the recurring players in patterning systems is the symmetry-disrupting morphogen gradient. This gradient gives rise to broad regions that are refined through the action of a variety of transcriptional regulators. In plants, many transcriptional regulators that influence developmental patterns have been identified through molecular genetic studies; uncovering morphogens, on the other hand, has been far more difficult. In this study, we provide evidence that the phytohormone auxin acts as a morphogen directing regional patterning in the developing gynoecium of *Arabidopsis thaliana*.

Auxin, historically the first plant hormone studied, has wide-ranging effects on growth and development throughout the plant. The major naturally occurring auxin in higher plants is indole-3-acetic acid (IAA), which is synthesized in the aerial portion of the plant and transported basipetally. According to the canalization hypothesis, a positive feedback mechanism focuses the flow of auxin into distinct cellular files, which will subsequently differentiate as veins (Sachs, 1991). The self-organizing aspect of this process requires directed auxin flow, proposed to be mediated by polar localization of auxin efflux carriers. Recently identified candidates for such carriers are restricted within the cell membrane in a cytoskeleton-dependent manner (Chen et al., 1998; Galweiler et al., 1998; Luschnig et al., 1998; Muller et al., 1998; Steinmann et al., 1999; Utsuno et al., 1998). Polar auxin transport (PAT) inhibitors have been utilized for decades to interfere with polar auxin flow, either by directly competing with auxin for carrier-binding or by otherwise rendering the cell incapable of transport (Tavares, 1973). Application of such inhibitors results in accumulation of auxin near source cells and depletion of auxin in cells normally downstream of the transport. Thus, treatment with PAT inhibitors increases the slope of existing auxin gradients in an inhibitor concentration-dependent manner. Studies of plants germinated on PAT inhibitor-containing media support a substantial role for auxin flux throughout plant development, and reveal a particularly strong effect of disrupted auxin flow on floral organ number and patterning (Okada et al., 1991). These studies are limited, however, by the finding that floral meristem initiation is largely dependent on proper PAT. Inhibitor-treated plants rarely make flowers. Studies of transgenic plants ubiquitously expressing IAA hydrolase, decreasing overall auxin levels, also demonstrate the dependence of flower meristem formation on IAA (Oka et al., 1999). The overall strong effects on plant morphology combined with the scarcity of flowers in these treatments makes assessment of auxin-transport-related floral organ defects difficult.

Although much work has been done to define the timing and mechanisms controlling the partitioning of the floral meristem into its constituent organs, the process of organ morphogenesis

remains poorly understood. *Arabidopsis* flowers consist of four organ types: the leaf-like perianth organs, sepals and petals, and the gametophyte-producing stamens and gynoecia. The gynoecium, the female reproductive structure, is perhaps the most complex organ formed by *Arabidopsis*, and has been meticulously observed throughout its ontogeny (Sessions, 1997). Genetic studies have yielded important insights into the underlying mechanism of patterning in the gynoecium. Several mutants affect specific subsets of the morphologically and functionally distinct tissues apparent in the mature gynoecium, suggesting that the development of individual tissues may be largely uncoupled (Alvarez and Smyth, 1999; Bowman and Smyth, 1999; Roe et al., 1997; Sessions and Zambryski, 1995).

Phenotypic analyses of one mutant, *ettin* (*ett*), facilitate the dissection of regional patterning during gynoecium organogensis. *ett* mutants display an allele-strength-dependent loss of valve tissue with a concomitant increase in apical/adaxial style and stigma and basal internode (Sessions and Zambryski, 1995). It has been proposed that the morphological defects in *ett* are caused by destabilized regional boundaries positioned at the apical and basal limits of the valves, resulting in an overall loss of valve and gain of flanking tissues (Sessions, 1997). The molecular nature of the ETT protein has important implications for the mechanism underlying the process of regional patterning. ETT shares a large amino-terminal DNA-binding domain with the auxin response factor (ARF) family of transcriptional regulators (Sessions et al., 1997). The founding member of this family, ARF1, was identified by its ability to bind a synthetic auxin response element (AuxRE) derived from conserved elements in the regulatory regions of many auxin-responsive genes (Ulmasov et al., 1997a). Ten ARFs have been characterized to date, with some acting as powerful activators of transcription and others as repressors (Ulmasov et al., 1999a,b). All but ETT display two islands of carboxy-terminal similarity which allow for protein-protein interactions both between ARF family members and with one group of auxin responsive genes, the Aux/IAAs (Kim et al., 1997; Ulmasov et al., 1999a). DNA-binding by some ARFs is disrupted by interaction with Aux/IAA proteins (Ulmasov et al., 1997b). None of the ARFs tested to date, including *ETT*, are inducible by exogenous application of auxin (Ulmasov et al., 1999b; J. L. N., L. J. F. and P. C. Z., unpublished results). Another developmental mutant, *spatula* (*spt*), is epistatic to *ett* in double mutant analysis and has been proposed as a potential downstream target of ETT (Alvarez and Smyth, 1998). *spt* is characterized by reduction of style and stigma, absence of transmitting tract cells and incomplete fusion of the apical end of the gynoecium. The recent cloning and characterization of the *SPT* promoter has revealed the presence of several putative AuxREs (M. Heisler, M. Groszmann and D. Smyth, personal communication), suggesting a mechanism for the regulation of *SPT* by *ETT*.

Genetic evidence implicates auxin flux in determination of floral organ number and patterning. *pin-formed1* flowers, defective in auxin efflux, show decreased number of floral organs and a dramatic loss of valve tissue in the gynoecium of the few flowers formed (Bennett et al., 1995). These effects are similar to those seen in plants exposed to PAT inhibitors. Mutations in *PINOID*, a kinase implicated in auxin transport or perception (Bennett et al., 1995; Christensen et al., 2000), and *MONOPTEROS* (ARF5) (Hardtke and Berleth, 1998; Przemeck et al., 1996) also cause substantial reduction in gynoecium valves. These mutants, as well as the PAT inhibitor studies, strongly implicate auxin in the specification of regional patterning early in gynoecium development.

Our study uses a novel technique of transiently applying a PAT inhibitor, N-1-naphthylphthalamic acid, to developing flowers to further characterize the role of auxin in gynoecium development. PAT inhibitors have marked effects on regional specification in wild-type gynoecia, as defined by morphological and histological landmarks for regional boundaries, as well as tissue-specific reporter lines. In addition, application of different concentrations of the inhibitor reveal an increased sensitivity of weak *ett* alleles to disruptions in PAT. A model suggesting an apical-basal gradient of auxin during gynoecium development is proposed. This model provides a mechanism linking ETT's putative transcriptional regulation of auxin-responsive genes to the establishment or elaboration of tissue patterning during gynoecial development.

MATERIALS AND METHODS

Stocks

The *ett-1*, *ett-2*, *spt-2* mutations have been described previously (Sessions and Zambryski, 1995; Alvarez and Smyth, 1999). Both *ett* alleles are in the Wassilewskija ecotype. *spt-2* is in the Landsberg *erecta* background. Wild-type Wassilewskija plants were used in mock treatments. The GT142 (Landsberg *erecta*) (Sundaresan et al., 1995) and SLG::GUS (Columbia) (Toriyama et al., 1991) lines have been described previously.

Polar auxin transport inhibitor treatments

Plants were grown under long day conditions (16 hour light, 8 hour dark) until flowering was visibly apparent (approximately 3.5 weeks). Plants were sprayed with a heavy mist of 10 or 100 μM N-1-naphthylphthalamic acid (Uniroyal Chemical Co., Inc.) with 0.01% Silwet L-77 (a surfactant; Lehle Seeds) at 9 am. Plants were then placed in humid chambers, returned to their regular light regime, resprayed at 4 pm, and returned to the humid chambers overnight. At 10 am the following day, plants were washed with a saturating spray of distilled water before being returned to the greenhouse. Mock treatments were performed with distilled water containing 0.01% Silwet L-77. Flowers were observed directly and fixed for histological and ultrastructutral analyses approximately 10-14 days after treatment.

Scanning electron microscopy

Samples for scanning electron microscopy analysis were fixed in FAA (3.7% formaldehyde, 5% glacial acetic acid, 50% ethanol) containing 1% Triton X-100, dehydrated in a graded ethanol series, and critical point dried with liquid CO_2. Tissues were coated with gold or gold/palladium and viewed using an ISI-DS130 microscope (International Scientific Instruments, Inc.) with an accelerating voltage of 10 kV.

β-glucuronidase (GUS) staining

Lines were grown under long day conditions, and control or NPA treatments were performed once flowering was evident (as described above). Apices were removed and placed immediately in an ice-cold solution containing, 0.1 M sodium phosphate (pH 7), 0.3% Triton X-100, 5 mM $K_3Fe(CN)_6$, 5 mM $K_4Fe(CN)_6$, 20% methanol, 0.3% X-glucuronic acid. After 5 minutes of vacuum infiltration, samples were placed at 37°C for 12 hours. Apices were then fixed in ice-cold FAA overnight and subsequently dehydrated in a graded ethanol series.

Light microscopy

Whole apices were fixed in FAA overnight at 4°C, washed for 2 hours in 0.1 M potassium phosphate buffer (pH 7.5), and then transferred to 8 N NaOH for 16 hours with agitation. Tissues were washed for 1 hour with 0.1 M potassium phosphate buffer (pH 7.5) and stained in 0.1% Aniline Blue in the same buffer solution for 15 minutes. Gynoecia were mounted on slides and viewed with Nomarski optics on a Leica DMRB microscope.

RESULTS

Transient disruption of polar auxin transport in the floral apex

N-1-naphthylphthalamic acid (NPA) is a phytotropin. This class of polar auxin transport inhibitors is defined by their structure, benzoic acid derivatives ortho-linked to aromatic ring systems (Lomax et al., 1995). Unlike other PAT inhibitors, which compete directly with auxin for transporter binding, phytotropins bind to another plasma membrane-localized protein thought to regulate the efflux carrier by an unknown mechanism. Several candidate targets for NPA-binding have been isolated biochemically, but the identity of these proteins and their connection to auxin transport are unknown (Lomax et al., 1995). *tir3*, an NPA resistant mutant, has fewer NPA binding sites (Ruegger et al., 1997) and may be a mutation in the NPA-binding protein or a factor necessary for its proper expression, localization, or stabilization. NPA has dramatic effects on plant growth and development and displays no auxin-like properties (Mattsson et al., 1999; Lomax et al., 1995).

NPA is not trafficked by the auxin efflux carrier, and appears to remain in the initial cells where it is introduced (Reed et al., 1998; Thomson et al., 1973). Several studies have successfully used NPA to disrupt PAT and analyze development (Mattsson et al., 1999; Okada et al., 1991). Flower development can be divided into three phases: initiation of floral meristems, initiation and patterning of floral organs within the floral meristem, and postfertilization seed set and fruit development. Assays directly addressing auxin's role in the first (Reinhardt et al., 2000) and last (Vivian-Smith and Koltunow, 1999) of these stages have been described. While effects throughout flower development are observed following the NPA treatments described in this work, the focus is to define the effects of NPA treatment on the second stage of flower development – morphogenesis of floral organs. Since prolonged NPA exposure severely restricts the number of flowers formed, in this investigation NPA was applied transiently to plants that have already initiated flowering. Plants were exposed to NPA for a single day and then washed thoroughly. Using the transient treatment described here, approximately ten flowers show defects in floral organ patterning.

Before treatment with NPA, the inflorescence meristem is a flattened dome tightly encircled by many flowers of varying developmental stages (Fig. 1A). After NPA treatment, the inflorescence meristem takes on a more tapered shape, and fewer early stage floral meristems are observed (Fig. 1B-E). The early stage floral meristems that are present show sepals aberrant in number and morphology from day 3 through day 7 (Fig. 1B-D). The inflorescence meristem recovers over time. By day 13, the meristem has resumed its wild-type appearance and initiation of floral meristems, verifying the transient nature of the NPA treatments (Fig. 1G). By day 19 post NPA treatment, a tight cluster of floral meristems may once again

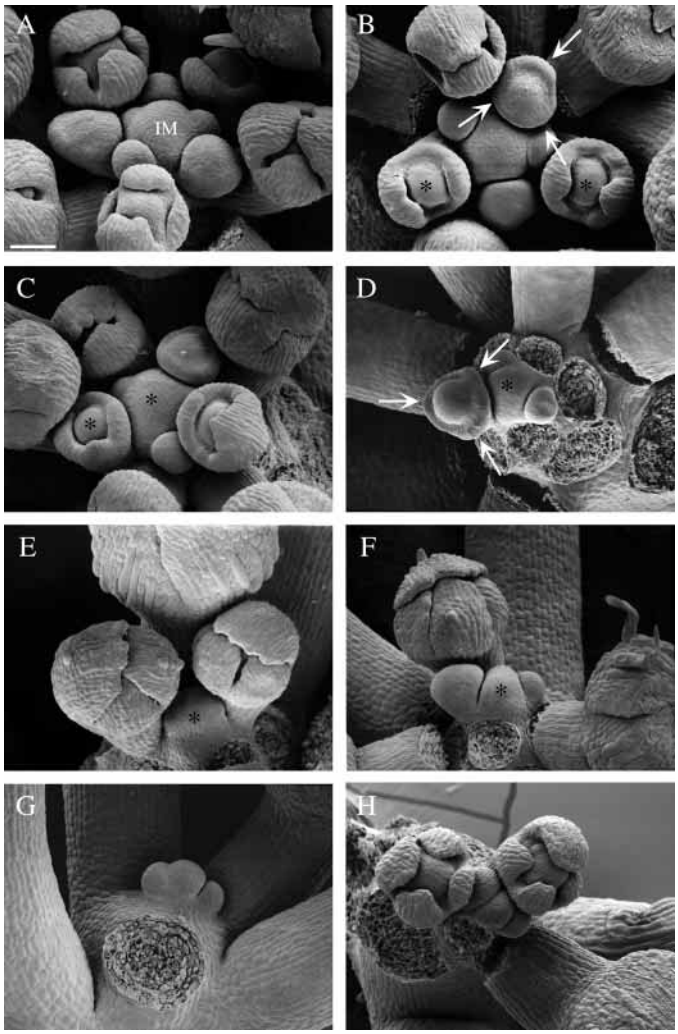

Fig. 1. Effects of NPA treatment. The oldest flowers, probably those present prior to NPA treatment show defects in silique elongation. These are followed by an average of ten flowers with defects in organ number and patterning. The final flowers made by the plant appear indistinguishable from those on mock-treated plants. (A-H) Scanning electron micrographs showing time course of NPA effects on inflorescence meristems. White arrows indicate aberrant sepal initiation. Asterisk denotes tapered meristems (both inflorescence and floral meristems are affected). (A) 1 day post-NPA treatment. (B) 3 days post-NPA treatment. (C) 5 days post-NPA treatment. (D) 7 days post-NPA treatment. Note reduction in number of floral meristems initiated. (E) 9 days post-NPA treatment. Note absence of primordia on inflorescence meristem (*). (F) 11 days post-NPA treatment. While the inflorescence meristem (*) remains aberrantly tapered, floral meristem initiation has resumed. (G) 13 days post-NPA treatment. The inflorescence meristem has returned to wild-type morphology and regular initiation of floral meristems. The large pedicels observed encircling the inflorescence meristem are from flowers initiated prior to day 9. (H) 19 days post-NPA treatment. The meristem is once again tightly encircled by floral meristems of varying stages. At all time points, mock-treated apices were indistinguishable from those in A (data not shown). Scale bar, 80 μm for all panels.

be observed (Fig. 1H). Another PAT inhibitor, 2,3,5-triiodobenzoic acid, was also used to confirm that the effects seen were a result of decreased polar auxin transport and were not NPA specific (data not shown). All subsequent analyses reported below were performed on flowers formed in the period after day 1 (Fig. 1B) and prior to day 11 (Fig. 1F) following NPA treatment.

NPA affects wild-type flower development

All whorls are affected by treatment with NPA

All floral organ types are affected by treatment with 100 μM NPA. In wild-type organ development, there is remarkably little variation in the number of organs formed. In the outer whorl organs of sepals, petals and stamens, NPA treatments expand the variation in organ number considerably (Fig. 2; see below for discussion of NPA effects on *ett* flowers). There is a general trend towards reduction of organ number, which is most pronounced in stamens. Sepals and petals often appear narrower than in the wild type, and anthers are frequently misformed (data not shown). These phenotypes mimic those observed in *pin-formed1* flowers (Bennett et al., 1995; Okada et al., 1991). Overall, the organs of the outer three whorls provide relatively few landmarks for characterizing aberrations in their form. Below we address the effects of PAT disruption on regional patterning in the gynoecium.

NPA has dramatic effects on gynoecium development

Several regions can be clearly distinguished in mature *Arabidopsis* gynoecia. These regions are, from apical tip to base: stigma, style, ovary, and short internode or stipe (Fig. 3A). Ovules are enclosed by the ovary wall, or valve, and connected to it through the placenta. *Arabidopsis* gynoecia comprise two congenitally fused carpels, forming two locules, each containing two strands of intercalating ovules along their length. The region between the two valves is defined as medial, and can be distinguished by a zone of cells, collectively termed the replum, which externally form a furrow running the length of the ovary.

Floral development has been divided into 20 stages, from floral meristem initiation in stage 1 to mature seeds falling from the dried fruit in stage 20 (Smyth et al., 1990). In floral stage 6, the gynoecium emerges from the center of the floral meristem as a slotted cylinder. During development, the cylinder grows upward (apically) and also inward (adaxially), initiating replum development. Ovules begin to differentiate in floral stage 8. Regional epidermal differences distinguishing valve and style become apparent just prior to medial fusion in floral stage 10. Stage 11 is characterized by the initiation of stigmatic papillae. By the completion of stage 12, all organs of the flower are fully mature, and the bud opens.

Treatment with 10 μM NPA results in subtle changes in the distribution of gynoecial tissues, observed as a slight reduction

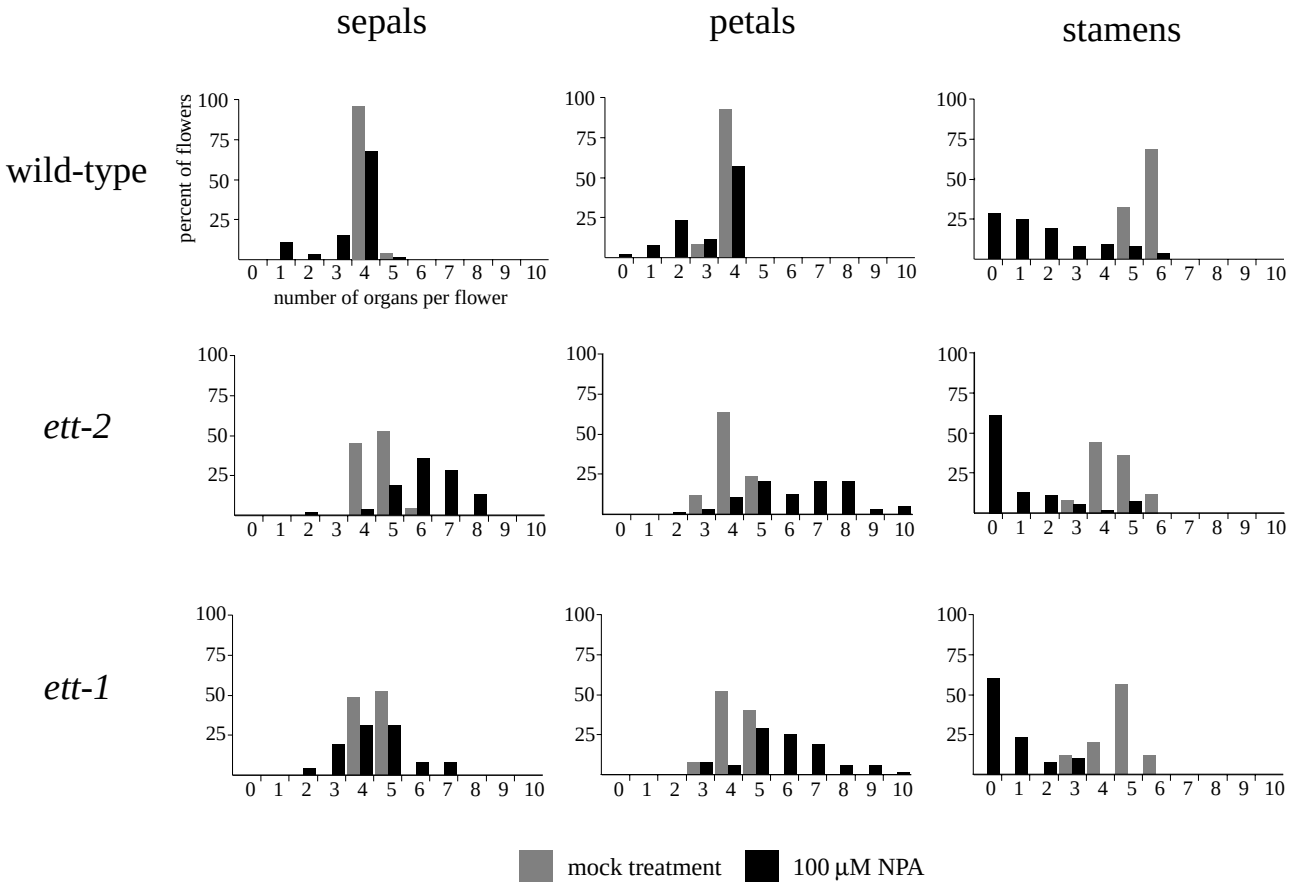

Fig. 2. Floral organ number counts following control and NPA treatments. Organ counts were performed 10-14 days following NPA treatment. Aberrant gynoecia were used to identify flowers affected by NPA treatment. In all mock treatments, 25 flowers were counted. In NPA treatments, 53 flowers were counted on 6 wild-type plants, 54 flowers on 6 *ett-2* plants and 52 flowers on 6 *ett-1* plants.

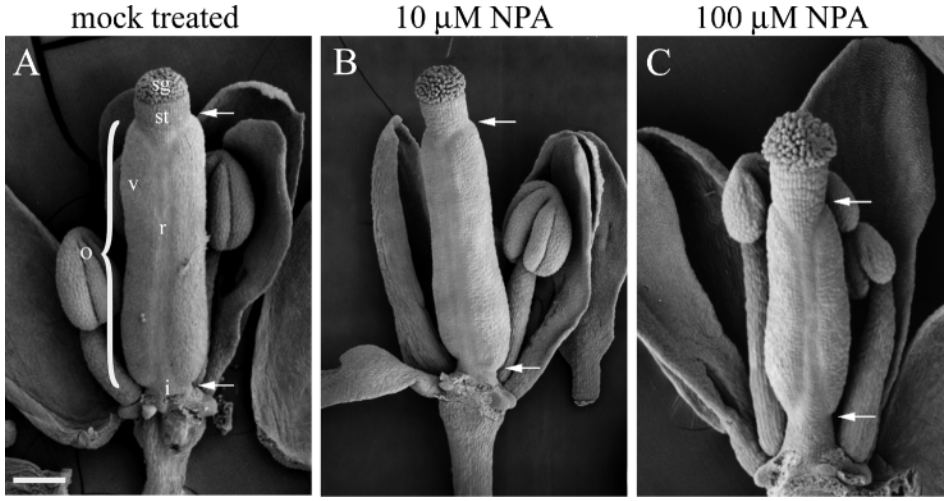

Fig. 3. Scanning electron micrographs showing NPA effects on tissue distribution in the wild-type gynoecium. Valve extent is indicated for the right side of each gynoecium as the space between the two white arrows. Late stage 12 gynoecia are shown for each treatment. (A) Mock-treated flower with stigma (sg), style (st), ovary (o), valve (v), adaxial replum (r), and stipe (i) indicated. (B) 10 μM NPA treatment. Note that the stigma and style are slightly elongated. (C) 100 μM NPA treatment. Note the reduced height of the gynoecium; the valves are smaller than in mock-treated plants, and there is a marked increase in style and stigma proliferation. Scale bar, (A) 165 μm, (B) 200 μm, (C) 140 μm.

in ovary length and a concomitant increase in stigma and style (Fig. 3B). With 100 μM NPA treatment, effects are more dramatic, revealing reduction of ovaries, including shrinkage of the valve in both the longitudinal and radial axes (Fig. 3C). In addition, stigmatic papillae, style, and stipe show increased elongation.

The epidermal cells of each region of the gynoecium display a distinct morphology (Fig. 4A,C). Style cells are rectangular and elongated along the apical/basal axis. Valve cells are smaller and more square. Medial furrow cells are still smaller than valve cells. Treatment with NPA does not affect the identity of the cells from each region (Fig. 4B). However, while the medial furrow in wild-type gynoecia is indented relative to the valves, the region between the valves protrudes outward in gynoecia treated with 100 μM NPA (Fig. 4A compared with B). Cells in this region appear more axialized, and their protrusion from between the valves may result from changes in cell shape and diminished size of the valve. Medial outgrowths are also observed in untreated weak *ettin* mutants; however these outgrowths consist of cells displaying characteristics of the stylar transmitting tract (Fig. 4C; see also Sessions, 1995).

NPA induced changes in epidermal morphology are mirrored in vascular patterns

Wild-type gynoecia have four internal veins, two medial and two lateral. At the style/ovary boundary, two effects on vascular traces may be observed which serve as internal landmarks for this regional transition. First, the lateral veins terminate. Second, the medial veins bifurcate at this junction and large arrays of xylem elements are apparent within the stylar region (Fig. 5A). The proliferation of stylar xylem suggests a high concentration of auxin during its development. 10 μM NPA treatments produce only mild effects on the bifurcation of the medial vasculature and the termination of the lateral strands (Fig. 5B), consistent with the subtle effects on style and valve observed by SEM. Treatments with 100 μM NPA result in both of the vascular markers of style/ovary boundary becoming more deeply basalized (Fig. 5C). A significant loss of ovules is also seen with high level NPA treatments (Fig. 5C).

NPA also alters expression of gynoecial tissue-specific markers

GT142 is an enhancer line that marks the dehiscence zone along the margins of the valves, and visually delimits the valve area (Fig. 6A; Sundaresan et al., 1995). Wild-type, untreated gynoecia show stronger expression at their apical ends, although staining can be detected ringing the entire valve. Plants treated with 100 μM NPA and stained for β-glucuronidase (GUS) expression illustrate the decrease in valve in both the radial and longitudinal axes (Fig. 6B,C). In Fig. 6C,

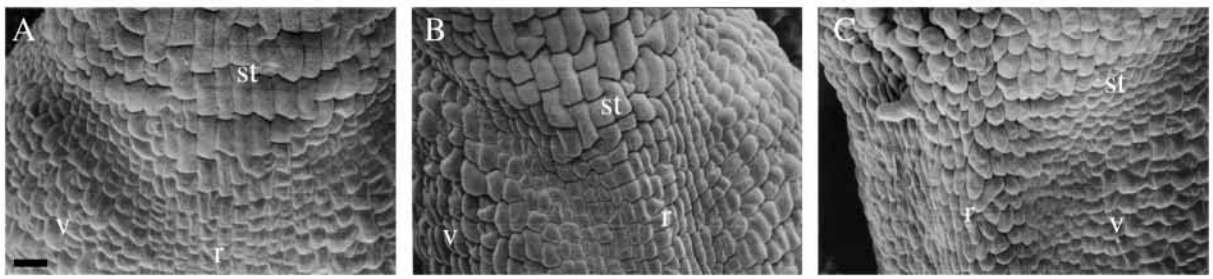

Fig. 4. Scanning electron micrographs of adaxial replum. (A) Junction of style (st), adaxial replum (r), and valve (v) in mock treated gynoecium. (B) Junction of style (st), adaxial replum (r), and valve (v) in 100 μM NPA-treated gynoecium. Note that cells are more axialized and grow out from between the valves, but retain other features of the adaxial replum. (C) Junction of style (st), adaxial replum (r), and valve (v) in *ett-2* gynoecium. Note medial outgrowth consists of bulbous cells, unlike any normally found on the surface of the gynoecium. Scale bar, 20 μm in all panels.

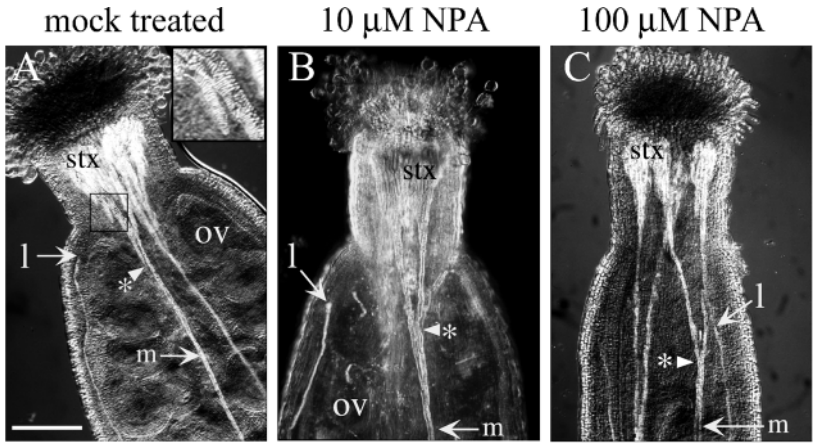

Fig. 5. Vascular patterning in cleared, whole-mount anthesis stage gynoecia. In each gynoecium, the medial (m) and lateral (l) bundles are indicated, as well as the stylar xylem (stx) which terminates the medial bundles. The point of bifurcation of the medial bundles is marked with an asterisk. A representative ovule is also indicated (ov) where present in A,B). (A) Mock treated gynoecium viewed medially. An enlarged view of xylem elements exhibiting characteristic cell wall thickenings is shown in the inset. (B) 10 μM NPA-treated gynoecium viewed medially. (C) An oblique view of 100 μM NPA treated gynoecium. Scale bar in lower left corner is 10 μm.

the gynoecium is viewed laterally and a particularly severe reduction in valve may be observed.

A second tissue-specific marker line uses the promoter of the S-Locus glycoprotein from *Brassica oleraceae* to direct GUS expression (Toriyama et al., 1991). Wild-type, mock-treated gynoecia show expression of GUS most strongly in the stigma (Fig. 6D,F). Treatments with 100 μM NPA cause GUS expression to be basalized (Fig. 6E). NPA treatments also provoke precocious expression of this stigmatic tissue marker (arrows in Fig. 6F compared with G). Mutations in *ett* also cause early appearance of stigmatic papillae when compared with wild type (Sessions, 1997).

NPA alters *ettin* mutant phenotypes

All whorls are affected by NPA treatment

ett affects all four whorls of the flower. In the outer three whorls, there are increases in perianth organ number and decreases in stamen number (Sessions and Zambryski, 1995). NPA treatments affect all organs of *ett* plants (Fig. 2). As in wild type, NPA treatments increase the variation in the number of sepals, petals and stamens produced. Stamen number is greatly reduced in all treated *ett* plants, and third whorl organs often consist of filamentous structures lacking anthers (Fig. 7B,E; st′). Mosaic organs composed of petal and stamen tissue are seen commonly in the second whorl (Fig. 7F; p′). Curling and wrinkling of the sepals is also apparent (Fig. 7C,E), and sepals are often reduced to filamentous structures (Fig. 7C; s′). This stochastic alteration in floral organ number and overall reduction in organ size is reminiscent of another mutant, *tousled* (*tsl*; Roe et al., 1997). *TSL* encodes a serine-threonine kinase which phosphorylates the C-terminal half of ETT in vitro (X. Liu, J. L. N., P. C. Z., and J. Roe, unpublished results). These results together may implicate *TSL* in the auxin response. Defects in gynoecium development caused by NPA treatments are also observed, and are described in detail below.

NPA enhances the gynoecium defect of weak *ett-2* alleles

ett-2 is a weak allele caused by a missense mutation that results in aberrant splicing of some transcripts (Sessions et al., 1997). *ett-2* gynoecia have reduced valves, expanded apical tissues, an elongated stipe, and a medial outgrowth composed of stylar tissue (Fig. 7A). Treatments with low levels of NPA (10 μM)

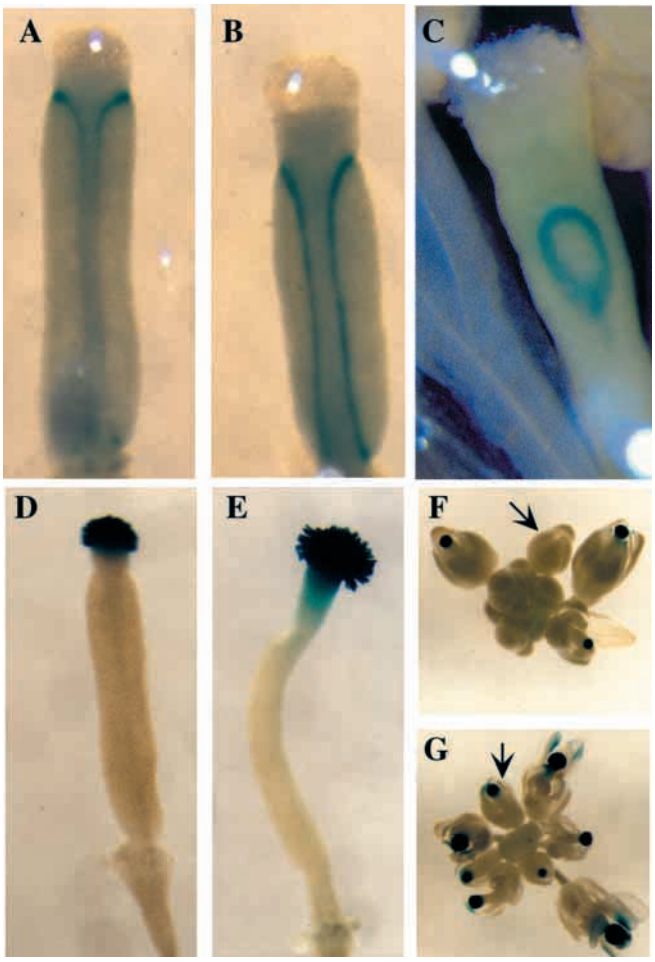

Fig. 6. Tissue-specific marker lines indicating changes in tissue distribution in NPA-treated gynoecia. (A) GT142 mock treated. The dehiscence zone at the edge of the valve appears blue. (B,C) 100 μM NPA-treated GT142. Note the reduction in overall size of the valves. (D,F) SLG::GUS mock treated. The apical tissues of the gynoecia, the style and stigma, appear blue. (E,G) SLG::GUS 100 μM NPA treated. The excessive (E) and precocious (G) proliferation of the stigma and style can be seen. Black arrows in F and G indicate flowers at the same stage of development; reporter expression can only be detected in G.

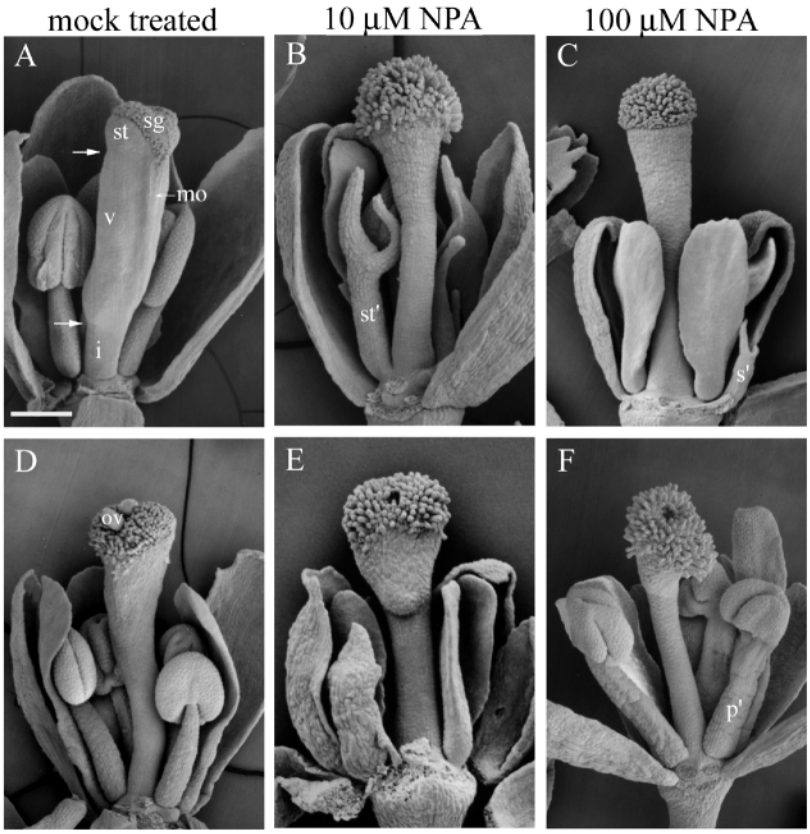

Fig. 7. Scanning electron micrographs showing NPA effects on tissue distribution in *ett* gynoecia. Stage 12/13 gynoecia are shown for each treatment. (A) *ett-2* mock-treated gynoecium with stigma (sg), style (st), valve (v), medial outgrowth (mo), and stipe (i) indicated. Valve extent is indicated on the left side of the gynoecium as the space between the two arrows. (B) *ett-2* gynoecium treated with 10 μM NPA. Stigmatic papillae are enlarged and are supported by elongated style and stipe tissue. No valve tissue is apparent. Note the increased height of the gynoecium relative to the petals, as compared with mock-treated *ett-2* (A). A misformed stamen lacking anther tissue in indicated (st′). (C) *ett-2* gynoecium treated with 100 μM NPA. The gynoecium is similar in appearance to that observed in the low level treatment (10 μM). Curling of the sepals is also evident. s′ indicates a bifurcated, filamentous sepal. (D) *ett-1* mock-treated gynoecium. An external ovule (ov) is indicated. No valve tissue is apparent. (E) *ett-1*gynoecium treated with 10 μM NPA. The overall structure is similar to mock-treated *ett-1*, except for the additional reduction in ovules. (F) *ett-1* gynoecium treated with 100 μM NPA. The high level treatment has no additional effect on *ett-1*. A mosaic second whorl organ composed of petal and stamen tissue is marked with a p′. Scale bar, (A) 250 μm, (B) 195 μm, (C) 205 μm, (D) 275 μm, (E) 190 μm, (F) 205 μm.

largely eliminate any apparent differentiation of valve tissue, and the remaining structure, composed exclusively of stigma, style and stipe, resembles that of strong *ett* alleles (Fig. 7B). This dramatic phenotype reveals *ett*'s increased sensitivity to NPA treatments, as low level NPA treatments have only subtle effects on development of wild-type gynoecia. 100 μM NPA treatments do not appear to further enhance these defects (Fig. 7C).

Gynoecial defects produced by strong *ett* alleles are largely unaffected by NPA treatment

ett-1 makes no detectable *ett* transcript, as a result of a T-DNA insertion near the beginning of the coding region (Sessions et al., 1997). *ett-1* gynoecia rarely make valves and consist solely of apical tissues supported by an elongated stipe (Sessions and Zambryski, 1995). Ovules are often exposed at the apical end of the structure. Treatments with 10 or 100 μm NPA result in only subtle enhancement of this exterior phenotype (Fig. 7E,F). The major effect of NPA treatments on *ett-1* is the severe reduction in the number of ovules produced (notice absence of external ovules in Fig. 7E,F compared with D). There are no apparent differences in the effects of low and high level NPA treatments.

Altered vasculature reflects altered regional boundaries

The basalization of medial vein bifurcation and lateral vein termination in *ett* mutants has been described previously (Sessions and Zambryski, 1995). In 10 μM NPA treated *ett-2* mutants, all vascular bundles branch at the apical end of the gynoecium, making it difficult to distinguish lateral from medial veins (Fig. 8B). If these veins are all medial, this would reflect complete basalization of medial bundle bifurcation and lateral bundle termination. In this case, medial veins would bifurcate at the base of the gynoecium, appearing as four strands instead of two, and lateral veins would not form at all. Alternatively, the phenotype observed with NPA-treated *ett*-2 gynoecia may be similar to what is observed with intermediate *ett* alleles where lateral veins take on medial vein attributes, bifurcating in medial bundle-like fans of xylem (Sessions and Zambryski, 1995). High level NPA treatments (100 μM) of *ett-2* plants produce large numbers of parallel veins that terminate at the top of the organ in a dramatically enhanced fan of xylem (Fig. 8C). No ovules are seen in NPA-treated *ett-2* gynoecia (Fig. 8B,C).

In *ett-1*, bifurcation of medial bundles and termination of lateral bundles is basalized, and the stylar xylem anastomoses at the apical end of the gynoecium (Sessions and Zambryski, 1995). These phenotypes are largely unaffected by 10 or 100 μM NPA treatments (Fig. 8E,F). As in treated *ett-2* plants, lateral veins are rarely observed in NPA-treated *ett-1* plants, and a clear bifurcation of the medial vasculature is not apparent. This may indicate an extremely basalized style/ovary boundary in these tissues. Overall, NPA-treated *ett-1* gynoecia show a very similar phenotype to NPA-treated *ett-2* gynoecia.

spt mutants are partially rescued by NPA treatment

Mutations in *SPATULA* (*SPT*) produce gynoecia with reduced apical tissues (Alvarez and Smyth, 1998; Alvarez and Smyth, 1999; see also Fig. 9A). *spt* gynoecia lack transmitting track cells and are often incompletely fused at the apical end. There is also reduced development of the stigmatic papillae. The

strong *spt* allele, *spt-2*, causes strikingly aberrant gynoecial vasculature (Fig. 9B). Instead of bifurcating at the style/ovary boundary, medial veins in *spt* gynoecia bifurcate at several points along the apical half of the valve and fan out abaxially. The stylar xylem is more extensively elaborated than in wild-type gynoecia. The lateral veins terminate in knots of xylem (Fig. 9B; l') and often curve adaxially. Discontinuous strands as well as isolated islands of xylem are also observed (data not shown).

While valve and internode tissues of *spt-2* gynoecia are less affected by treatment with 100 μM NPA than either *ett* or wild-type gynoecia, NPA largely suppresses the effects of the mutation on apical tissues (Fig. 9C). Stipe length is moderately increased and valves are slightly reduced. A majority of gynoecia show complete fusion of the apical end and greatly enhanced stigma development (Fig. 9C). Vasculature of the NPA-treated *spt-2* gynoecia is remarkably similar to that observed in untreated wild-type plants (Fig. 9D); the bifurcation of medial veins is more limited to the style/ovary boundary, and the stylar xylem arrays are less dense. Lateral vein knots are also reduced. Ovule number is reduced as in NPA treatments of wild type.

DISCUSSION

This work documents the effects of disrupted polar auxin transport on floral organ development, particularly regional differentiation in the *Arabidopsis* gynoecium. NPA treatments result in increased concentration of auxin near source cells and depauperation in outlying areas. In wild-type gynoecia, NPA treatment results in increased apical tissue proliferation, a basalized style/ovary boundary, decreased valve production and an elongated stipe. Ovule development also is negatively affected by NPA treatments. Analyses via scanning electron microscopy, tissue-specific GUS marker lines, and light microscopy on cleared tissue support these findings.

Low level NPA treatments are sufficient to strongly enhance the gynoecial phenotype produced by the weak *ett-2* allele – drastically reducing valve, increasing both proliferation and distribution of apical tissues, and increasing the length of the stipe. The exterior morphology of plants with the strong *ett-1* allele is not dramatically affected by NPA treatments, though apical tissues proliferate more than in mock treated *ett-1* plants. As in wild type, ovule production in *ett* gynoecia is severely limited by NPA treatment. In contrast, *spt* gynoecia are partially rescued by NPA treatment. These results uncover an intimate link between the action of *ETT* and *SPT* and normal polar auxin transport in the gynoecium.

The gynoecium as modified leaves: evolutionary and developmental parallels

In leaf development, the prevailing model for vein initiation is that auxin is first synthesized in leaf margins and subsequently drains away towards the center of the organ. The flow of auxin is canalized into discrete channels which then differentiate into a network of veins (Mattsson et al., 1999; Sachs, 1991). Loss of polar auxin transport in developing *Arabidopsis* leaves, resulting from mutations in *PIN1* or following NPA treatments (Mattsson et al., 1999), supports this model and shows striking parallels with the results in the gynoecium described here. Young leaves treated with NPA exhibit increased density of veins along their margins, as well as multiple parallel midveins. It is proposed that reduced PAT causes auxin to pool at the margins, leading to increased vein production there. Depleted auxin at the midvein would disrupt canalization and produce multiple smaller veins connecting the leaf to the petiole. This

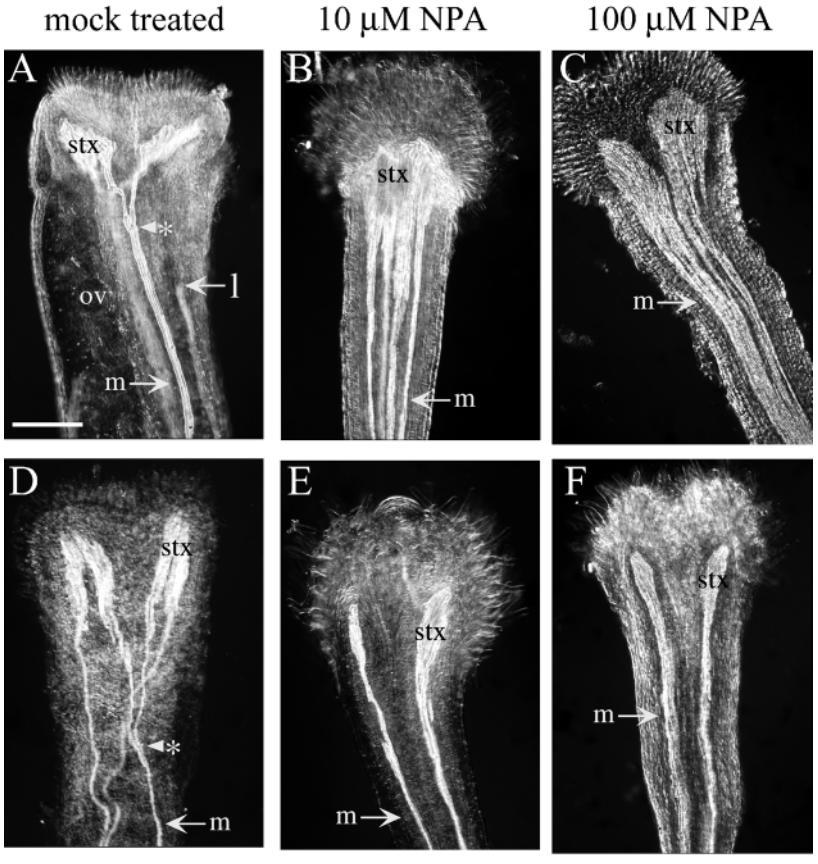

Fig. 8. Vascular patterning in cleared, whole-mount anthesis stage gynoecia. In each gynoecium, the medial (m) and lateral (l) bundles are indicated where present, as well as the stylar xylem (stx) which terminates the medial bundles. The point of bifurcation of the medial bundles is also indicated where present (*). A representative ovule (ov) is indicated in A, the only case where ovules are observed. (A) *ett-2* mock-treated gynoecium. (B) *ett-2* gynoecium treated with 10 μM NPA. Though four bundles are present, it is difficult to distinguish medial from lateral as all veins terminate in medial bundle-like fans of xylem. (C) *ett-2* gynoecia treated with 100 μM NPA. Notice many parallel veins terminating in large fans of xylem. (D) *ett-1* mock-treated gynoecia. The medial bundles anastomose at the apical end of the gynoecia. (E) *ett-1* gynoecium treated with 10 μM NPA. Only two bundles are observed, both showing medial attributes. (F) *ett-1* gynoecium treated with 100 μM NPA. These gynoecia closely resemble those of *ett-1* gynoecia treated with 10 μM NPA. Scale bar, 10 μm.

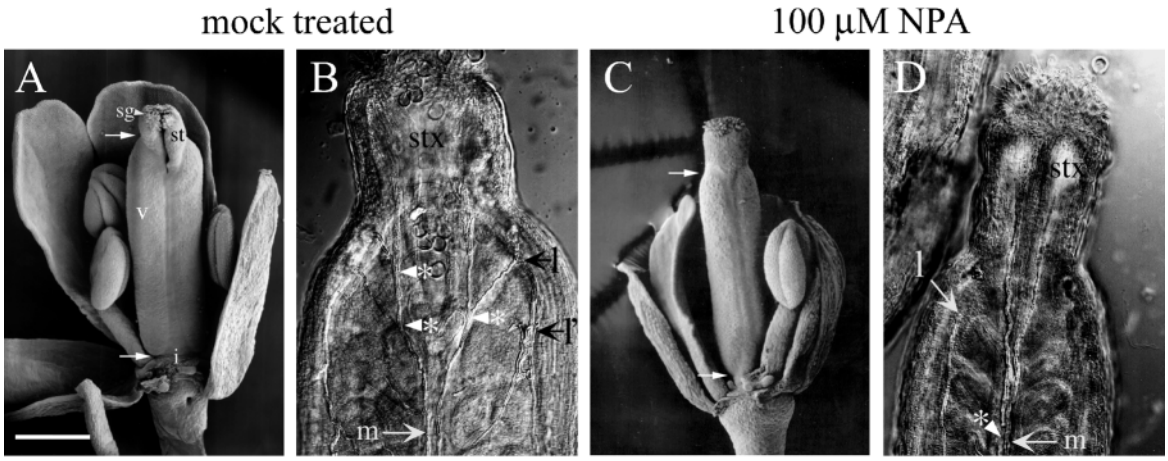

Fig. 9. NPA effects on tissue distribution in *spt* gynoecia. Stage 12/13 gynoecia are shown in all panels. (A,C) Scanning electron micrographs are shown for both treatments. (B,D) Vascular patterning in cleared, whole-mount gynoecia. The medial (m) and lateral (l) bundles are indicated, as well as the stylar xylem (stx). The point(s) of bifurcation of the medial bundles is marked with an asterisk. (A) Mock-treated *spt-2* gynoecium with stigma (sg), style (st), valve (v), and stipe (i) indicated. Note the lack of fusion at the apical end and underdeveloped stigmatic papillae. (B) Mock-treated *spt-2* gynoecium. Note the multiple bifurcations of the medial veins and the knot of xylem near the terminus of the lateral vein (l'). (C) *spt-2* gynoecium treated with 100 μM NPA. The internode is only slightly elongated and the valves show only modest reductions following NPA treatment. The apical tissue phenotypes are largely suppressed – the style appears completely fused and stigmatic papillae are more elongated and abundant. (D) *spt-2* gynoecium treated with 100 μM NPA. The vascular defects are almost completely suppressed by NPA treatment. The traces appear more focused overall, with fewer bifurcations, discontinuous strands, and isolated xylem elements. There are also dramatic reductions in the xylem knots at the termini of lateral veins. Medial vein bifurcation and lateral vein termination are somewhat basalized as in wild-type NPA treated gynoecia. Scale bar, (A) 375 μm, (B) 10 μm, (C) 300 μm, (D) 10 μm.

is similar to NPA effects on the gynoecium where the veins linking the gynoecium to the receptacle are multiplied. This pattern of venation is consistent with cells along the style/ovary boundary acting as a source of auxin. Veins in NPA-treated gynoecia are strikingly similar to those observed in *pinoid* (Christensen et al., 2000), as well as *ett*. In light of the aberrant venation found in *spt* gynoecia, these observations imply a central role for auxin in gynoecium morphogenesis. The Angiosperm carpel is proposed to have originated as modified leaves which fused to enclose and protect the gametophyte, suggesting that these parallel effects observed in leaf and gynoecium development may reflect a common evolutionary program.

Auxin as a morphogen patterning the gynoecium

Morphogens directly trigger differential responses in a short-range, concentration-dependent manner. Recent studies have concluded that auxin fits many of the criteria for a morphogen, including work in pine and aspen where a short-range auxin gradient over the lateral meristem acts as a positional cue for cambial growth (Tuominen et al., 1997; Uggla et al., 1998; Uggla et al., 1996). Analyses of *Arabidopsis* roots strongly suggests that auxin is a key organizer of cellular patterning in that tissue (Sabatini et al., 1999). We propose a model where auxin acts as a morphogen patterning the gynoecium (Fig. 10). The dramatic shifting of regional boundaries caused by NPA treatment, may be explained by an apical-basal gradient of auxin early in development. In this model, two boundaries in the gynoecium primordium (a and b) mark threshold levels of auxin. One boundary lies between presumptive style (dark green) and valve (light green); the other boundary separates presumptive valve and stipe (yellow). Auxin-producing cells are proposed to reside in the apical end of the gynoecium primordium, represented as the wide base of the triangle shown to the left of each panel. Treatment with NPA results in pooling of auxin in these primordium cells, promoting precocious and excessive proliferation of apical tissues in the mature gynoecium (shown as dark green in schematics below primordia). The depletion of auxin in more basal primordium cells results in the loss of valve and ovules (light green) and lengthening of the stipe (yellow) in the mature gynoecium. This decrease in auxin transport is represented as a triangle with decreased length in Fig. 10B, bringing 'a' and 'b' threshold levels closer together. NPA studies and analyses of auxin transport mutants show that valve development requires proper PAT. In our model, valve formation is promoted by mid-level auxin concentrations. The stipe may be the default developmental program resulting from little or no auxin.

The model described above addresses the effects of auxin on longitudinal development of the gynoecium. It is clear, however, that auxin significantly affects radial development as well, most clearly seen in the replum and valve. Several gynoecium mutants display defects in both axes of the gynoecium, suggesting that their development is likely coordinated. *tousled*, *crabs claw* and *spt* all show defects in carpel fusion and reduced apical tissue production (Alvarez and Smyth, 1999; Bowman and Smyth, 1999; Roe et al., 1997). *ett* gynoecia show an eversion of stylar transmitting tract, in addition to the apical-basal defects previously mentioned (Sessions and Zambryski, 1995).

Another possible site of auxin action is during ovule development. The initiation or resumption of meristematic activity in the placenta likely involves alterations in local hormone ratios. Ovules are more sensitive than other tissues of the gynoecium to disruptions in PAT, as valves produced in treated wild-type plants are largely devoid of ovules. This loss

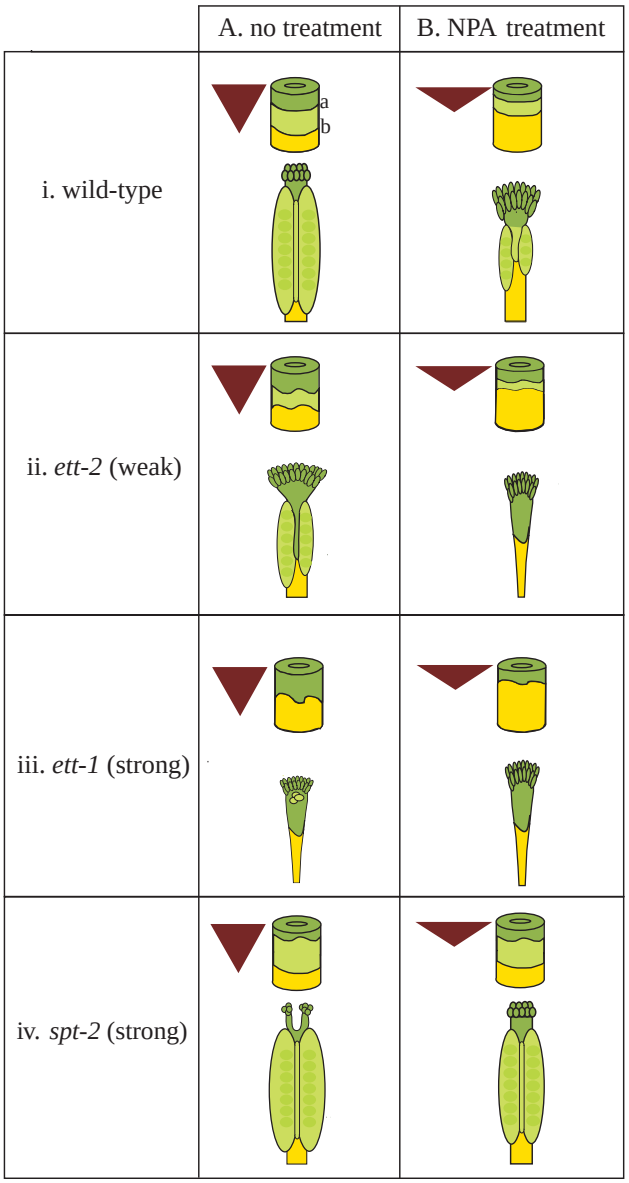

Fig. 10. Model of gynoecium development with auxin acting as a gradient-forming morphogen. Major regions of the gynoecium for wild type, weak *ett-2* and strong *ett-1* are indicated: dark green, style/stigma; light green, ovary; yellow, stipe. Triangles indicate relative concentration of auxin, as well as the direction of auxin flux. Cylinders represent gynoecium primordia. Horizontal lines, a and b, within the primordium represent emerging regional boundaries dependent upon defined auxin concentrations. Wavy horizontal lines in the primordia of *ett* mutants represent destabilization of these boundaries, as a result of reduced ETT function. Schematics below the primordia represent the mature structures resulting from the conditions present early on in development. (A) Models for development in the absence of NPA treatment in wild type (i), *ett-2* (ii), *ett-1* (iii), and *spt-2* (iv). (B) With NPA treatment, the slope of the auxin gradient is increased. This is represented as a decreased length of the auxin concentration triangle. This alteration results in higher auxin concentrations at the apical end of the structure and depletion of auxin at the base. The increase in auxin concentration at the apical ends results in increased apical tissue proliferation, most notably in wild type and *ett-2*. The change in the slope of auxin concentration brings the regional boundaries dependant on threshold levels of auxin closer together. In the weak *ett-2* allele (ii), this decreased area of the presumptive valve region is further compromised by destabilized boundaries. As a result, the light green region of the primordium is greatly reduced and valves are rarely observed in mature gynoecia. This effect resembles strong *ett-1* gynoecia (Aiii). Strong *ett-1* gynoecia (iii) are relatively unaffected by treatment with NPA. *spt* mutants are defective in apical tissue development, represented as a wavy apical line in the primordia. The presumed pooling of auxin in the apical tissues caused by NPA treatments is able to partially compensate for the effects of the *spt-2* mutation, perhaps by bypassing a weakened auxin response (iv). The reduced sensitivity of *spt* gynoecia to NPA treatment, relative to wild-type plants, is evident in the mild effects on valve and internode length. This may indicate that auxin signal transduction in the gynoecium is largely dependent upon a *SPT*-mediated pathway.

of ovules appears to be position-dependent, most severely affecting ovules at the apical end of the gynoecium (data not shown), perhaps reflecting an upper limit of local auxin concentrations for proper ovule development. However, *ETT* does not appear to play a large role in mediating the auxin response in the ovules, as these tissues are least affected by loss of *ETT*. *ett tsl* double mutants, in fact, leave a structure consisting solely of placenta and ovules, suggesting neither gene is required for these tissues to differentiate. As ETT is one of a large family of proteins, another ARF may mediate the auxin response in ovules.

As our model relies on auxin gradients for promoting regional patterning in the gynoecium, we attempted to determine the presence of auxin, and auxin gradients within the developing organ. Unfortunately, the best tools currently available – a monoclonal auxin antibody (Pence and Caruso, 1995) and the auxin-responsive reporter construct, DR5 (Ulmasov et al., 1997b) – were inconclusive (data not shown). The small size of the *Arabidopsis* gynoecium primordium and the limited sensitivity of available approaches make accurate quantitation of auxin levels difficult to determine.

ETT's role

ETT is proposed to establish or elaborate two regional boundaries defining the apical and basal ends of valves during gynoecium development, as illustrated in Fig. 10A (adapted from Sessions, 1997). That NPA treatments phenocopy many aspects of the *ett* phenotype, yet ETT is not itself auxin inducible, demonstrates that polar auxin transport is required at these same boundaries. In this model, ETT mediates the mid-level auxin response, specifying valve development, while restricting high level auxin responses, perhaps by binding to the promoters of auxin-responsive genes. Decreased level or function of ETT results in destabilized boundaries in the developing gynoecium (represented by wavy lines around threshold levels of auxin in Fig. 10Aii,iii). This destabilization results in a shrinkage of the presumptive valve region (light green) and expansion of the presumptive apical (dark green) and basal (yellow) regions in the primordium. Moderate basalization of the 'a' boundary and raising of the 'b' boundary causes the phenotype observed in weak *ett-2* gynoecia. In strong *ett-1* mutants, the shift in boundaries is more extreme, such that the middle region is eliminated.

The steeper auxin gradient resulting from NPA treatment brings the destabilized boundaries of *ett-2* still closer, phenocopying *ett-1*, resulting in a stochastic loss of valve

(Fig. 10Bii). NPA-treated *ett-2* gynoecia are largely indistinguishable from strong *ett-1* with two exceptions: loss of ovules and greater overall length. The latter may be attributed to an increased elongation of apical tissues caused by pooled auxin. According to this model, strong *ett* gynoecia, lacking ETT protein, already exhibit a severe reduction or elimination of the mid-level auxin response (Fig. 10Aiii). NPA treatment exacerbates this phenotype by expanding the apical tissues, eliminating any valve formation, and greatly interfering in ovule production (Fig. 10Biii).

ETT and *SPT*

In our model, polar auxin flux establishes a gradient of auxin concentration which ETT translates into regional boundaries. Weak *ett-2* mutants are enhanced by decreased auxin flux, but strong *ett-1* mutants are epistatic to the effects of NPA because they are unable to interpret the auxin gradient. The epistasis of *spt* over *ett* suggests that ETT may restrict apical tissue proliferation by negatively regulating *SPT*. The extreme alterations in vascular patterning in *spt* gynoecia may reflect a weakened response to auxin. Our model would predict that NPA treatment would result in pooling of auxin in apical cells, leading to increased proliferation of these cells, and partial suppression of the *spt* phenotype (Fig. 10iv), consistent with what is observed in NPA treatments of *spt-2*. In addition, the reduced sensitivity of *spt* gynoecia to NPA treatment, relative to wild-type plants, indicates that auxin signal transduction in this organ is largely dependent upon a *SPT*-mediated pathway. In light of previous work with PAT inhibitors and auxin mutants, these findings together illustrate the significant role auxin plays in patterning the *Arabidopsis* gynoecium.

We are indebted to Judy Roe and Allen Sessions for vision, advice and support. We thank Peter Repetti and Katrina Crawford for insightful review of this manuscript; Fred Hempel and the electron microscope facility for help with SEM, members of the Zambryski lab for useful discussions; the greenhouse staff for plant care; Denise Schichnes and Steve Ruzin of the Center for Biological Imaging for assistance and use of the facilities; June Nasrallah, Venkatesan Sundaresan, Yuval Eshed and John Bowman for providing seeds; Marcus Heisler and David Smyth for communicating results prior to publication. J. L. N. thanks Peter Repetti, Katrina Crawford and Carrie Cowan for wit and wisdom. J. L. N. is supported by the National Institute of Health Training Grant in Developmental Biology 5T32HD07375. This work also was supported by the Department of Energy grant DEFG03-88ER13882 to P. C. Z.

REFERENCES

Alvarez, J. and Smyth, D. R. (1998). Genetic pathways controlling carpel development in *Arabidopsis thaliana*. *J. Plant Res.* **111**, 295-298.

Alvarez, J. and Smyth, D. R. (1999). *CRABS CLAW* and *SPATULA*, two *Arabidopsis* genes that control carpel development in parallel with *AGAMOUS*. *Development* **126**, 2377-2386.

Bennett, S. R. M., Alvarez, J., Bossinger, G. and Smyth, D. R. (1995). Morphogenesis in *pinoid* mutants of *Arabidopsis thaliana*. *Plant J.* **8**, 505-520.

Bowman, J. L. and Smyth, D. R. (1999). *CRABS CLAW*, a gene that regulates carpel and nectary development in *Arabidopsis*, encodes a novel protein with zinc finger and helix-loop-helix domains. *Development* **126**, 2387-2396.

Chen, R., Hilson, P., Sedbrook, J., Rosen, E., Caspar, T. and Masson, P. H. (1998). The arabidopsis thaliana AGRAVITROPIC 1 gene encodes a component of the polar-auxin-transport efflux carrier. *Proc Natl Acad Sci USA* **95**, 15112-15117.

Christensen, S. K., Dagenais, N., Chory, J. and Weigel, D. (2000). Regulation of auxin response by the protein kinase PINOID. *Cell* **100**, 469-478.

Galweiler, L., Guan, C., A, M., Wisman, E., Mendgen, K., Yephremov, A. and Palme, K. (1998). Regulation of polar auxin transport by AtPIN1 in Arabidopsis vascular tissue. *Science* **282**, 2226-2230.

Hardtke, C. S. and Berleth, T. (1998). The Arabidopsis gene *MONOPTEROS* encodes a transcription factor mediating embryo axis formation and vascular development. *EMBO* **17**, 1405-1411.

Kim, J., Harter, K. and Theologis, A. (1997). Protein-protein interactions among the Aux-IAA proteins. *Proc. Natl. Acad. Sci. USA* **94**, 11786-11791.

Lomax, T. L., Muday, G. K. and Rubery, P. H. (1995). Auxin transport. In *Plant Hormones and their Role in Plant Growth and Development*, (ed. P. J. Davies), pp. 509-530. Boston Dordrecht (Netherlands): Kluwer Academic Publishers.

Luschnig, C., Gaxiola, R. A., Grisafi, P. and Fink, G. R. (1998). EIR1, a root-specific protein involved in auxin transport, is required for gravitropism in Arabidopsis thaliana. *Genes Dev.* **12**, 2175-2187.

Mattsson, J., Sung, Z. R. and Berleth, T. (1999). Responses of plant vascular systems to auxin transport inhibition. *Development* **126**, 2979-2991.

Muller, A., Guan, C., Galweiler, L., Tanzler, P., Huijser, P., Marchant, A., Parry, G., Bennett, M., Wisman, E. and Palme, K. (1998). AtPIN2 defines a locus of Arabidopsis for root gravitropism control. *EMBO J.* **17**, 6903-6911.

Oka, M., Miyamoto, K., Okada, K. and Ueda, J. (1999). Auxin polar transport and flower formation in Arabidopsis thaliana transformed with indoleacetamide hydrolase (*iaaH*) gene. *Plant Cell Physiol.* **40**, 231-237.

Okada, K., Ueda, J., Komaki, M. K., Bell, C. J. and Shimura, Y. (1991). Requirement of the auxin polar transport system in early stages of *Arabidopsis* floral bud formation. *Plant Cell* **3**, 677-684.

Pence, V. C. and Caruso, J. L. (1995). Immunoassay methods of plant hormone analysis. In *Plant Hormones and their Role in Plant Growth and Development*, (ed. P. J. Davies), pp. 240-256. Boston Dordrecht (Netherlands): Kluwer Academic Publishers.

Przemeck, G. K. H., Mattsson, J., Hardtke, C. S., Sung, Z. R. and Berleth, T. (1996). Studies on the role of the *Arabidopsis* gene *MONOPTEROS* in vascular development and plant cell axialization. *Planta* **200**, 229-237.

Reed, R. C., Brady, S. R. and Muday, G. K. (1998). Inhibition of auxin movement from the shoot into the root inhibits lateral root development in Arabidopsis. *Plant Physiol.* **118**, 1369-1378.

Reinhardt, D., Mandel, T. and Kuhlemeier, C. (2000). Auxin Regulates the Initiation and Radial Position of Plant Lateral Organs. *Plant Cell* **12**, 507-518.

Roe, J. L., Nemhauser, J. L. and Zambryski, P. C. (1997). TOUSLED participates in apical tissue formation during gynoecium development in *Arabidopsis*. *Plant Cell* **9**, 335-353.

Ruegger, M., Dewey, E., Hobbie, L., Brown, D., Bernasconi, P., Turner, J., Muday, G. and Estelle, M. (1997). Reduced naphthylphthalamic acid binding in the *tir3* mutant of *Arabidopsis* is associated with a reduction in polar auxin transport and diverse morphological defects. *Plant Cell* **9**, 745-757.

Sabatini, S., Beis, D., Wolkenfelt, H., Murfett, J., Guilfoyle, T., Malamy, J., Benfey, P., Leyser, O., Bechtold, N., Weisbeek, P. et al. (1999). An auxin-dependent distal organizer of pattern and polarity in the *Arabidopsis* root. *Cell* **99**, 463-472.

Sachs, T. (1991). Cell polarity and tissue patterning in plants. *Development: 91 Suppl.* **1**, 83-93.

Sessions, A., Nemhauser, J. L., McColl, A., Roe, J. L., Feldmann, K. A. and Zambryski, P. C. (1997). *ETTIN* patterns the *Arabidopsis* floral meristem and reproductive organs. *Development* **124**, 4481-4491.

Sessions, R. A. (1997). *Arabidopsis* (Brassicaceae) flower development and gynoecium patterning in wild type and *ettin* mutants. *Am. J. Bot.* **84**, 1179-1191.

Sessions, R. A. and Zambryski, P. C. (1995). *Arabidopsis* gynoecium structure in the wild type and in *ettin* mutants. *Development* **121**, 1519-1532.

Smyth, D. R., Bowman, J. L. and Meyerowitz, E. M. (1990). Early flower development in *Arabidopsis*. *Plant Cell* **2**, 755-767.

Steinmann, T., Geldner, N., Grebe, M., Mangold, S., Jackson, C. L., Paris, S., Galweiler, L., Palme, K. and Jurgens, G. (1999). Coordinated polar localization of auxin efflux carrier PIN1 by GNOM ARF GEF. *Science* **286**, 316-318.

Sundaresan, V., Springer, P., Volpe, T., Haward, S., Jones, J. D., Dean, C., Ma, H. and Martienssen, R. (1995). Patterns of gene action in plant development revealed by enhancer trap and gene trap transposable elements. *Genes Dev.* **9**, 1797-1810.

Thomson, K., Hertel, R., Muller, S. and Tavares, J. (1973). 1-N-Naphthylphthalamic Acid and 2,3,5-Triiodobenzoic Acid: in vitro binding to particulate cell fractions and action on auxin transport in corn coleoptiles. *Planta* **109**, 337-352.

Toriyama, K., Thorsness, M. K., Nasrallah, J. B. and Nasrallah, M. E. (1991). A *Brassica* S locus gene promoter directs sporophytic expression in the anther tapetum of transgenic *Arabidopsis*. *Dev. Biol.* **143**, 427-431.

Tuominen, H., Puech, L., Fink, S. and Sundberg, B. (1997). A radial concentration gradient of indole-3-acetic acid is related to secondary xylem development in hybrid aspen. *Plant Physiol.* **115**, 577-585.

Uggla, C., Mellerowicz, E. J. and Sundberg, B. (1998). Indole-3-acetic acid controls cambial growth in scots pine by positional signaling. *Plant Physiol.* **117**, 113-121.

Uggla, C., Moritz, T., Sandberg, G. and Sundberg, B. (1996). Auxin as a positional signal in pattern formation in plants. *Proc. Natl. Acad. Sci. USA* **93**, 9282-9286.

Ulmasov, T., Hagen, G. and Guilfoyle, T. J. (1997a). ARF1, a transcription factor that binds to auxin response elements. *Science* **276**, 1865-1868.

Ulmasov, T., Hagen, G. and Guilfoyle, T. J. (1999a). Activation and repression of transcription by auxin-response factors. *Proc. Natl. Acad. Sci. USA* **96**, 5844-5849.

Ulmasov, T., Hagen, G. and Guilfoyle, T. J. (1999b). Dimerization and DNA binding of auxin response factors. *Plant J.* **19**, 309-319.

Ulmasov, T., Murfett, J., Hagen, G. and Guilfoyle, T. J. (1997b). Aux-IAA proteins repress expression of reporter genes containing natural and highly active synthetic auxin response elements. *Plant Cell* **9**, 1963-1971.

Utsuno, K., Shikanai, T., Yamada, Y. and Hashimoto, T. (1998). Agr, an Agravitropic locus of Arabidopsis thaliana, encodes a novel membrane-protein family member. *Plant Cell Physiol.* **39**, 1111-1118.

Vivian-Smith, A. and Koltunow, A. M. (1999). Genetic analysis of growth-regulator-induced parthenocarpy in Arabidopsis. *Plant Physiol.* **121**, 437-451.